attenuated, but using the spectrometer as detector that has a spectral sensitive range between about 440 nm and 975 nm, this limitation is not such to prevent the exploitation of the experimental advantages offered by the use of the OPO as a single source for strong pump and Stokes waves in order to generate CARS on polystyrene (strong Raman resonance at 3060 cm^{-1}).

The spectral transmission characteristics of the used objectives have been measured in the region 900-1700 nm by means of a modified version of the set-up shown in Fig. 3.4, where an Optical Spectrum Analyzer (OSA, Agilent 86146B) in the NIR has been used as a diagnostic tool, instead of the Avaspec 2048. The two objectives show similar behaviour, with a transmittance that decreases in the region 900-1100 nm and a plateau in the 1100-1700 nm about 3 dB below the value at 900 nm. The focusing objective thus introduces differential attenuation: if signal and idler enter the objective with equal power, the output signal-to-idler power ratio will be about 2:1.

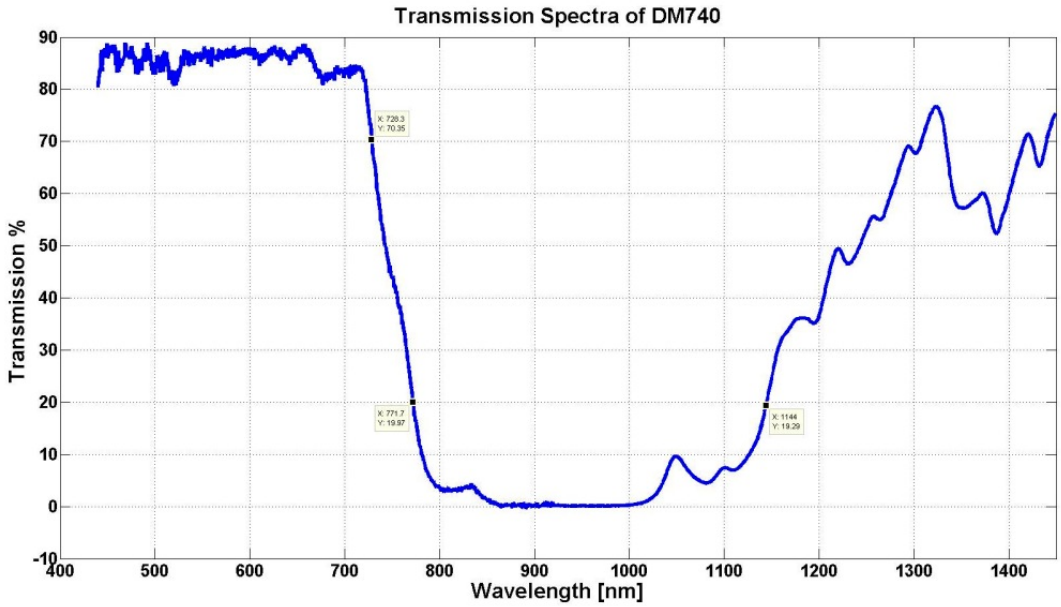

Fig. 3.5 Spectral transmittivity of the dichroic filter DM740 used in the experiment.

In order to control and get the characterization data of the optical component transmission the infrared region measured using the Optical Spectrum Analyzer (OSA, Agilent 86146B) a specific Labview program has been developed.

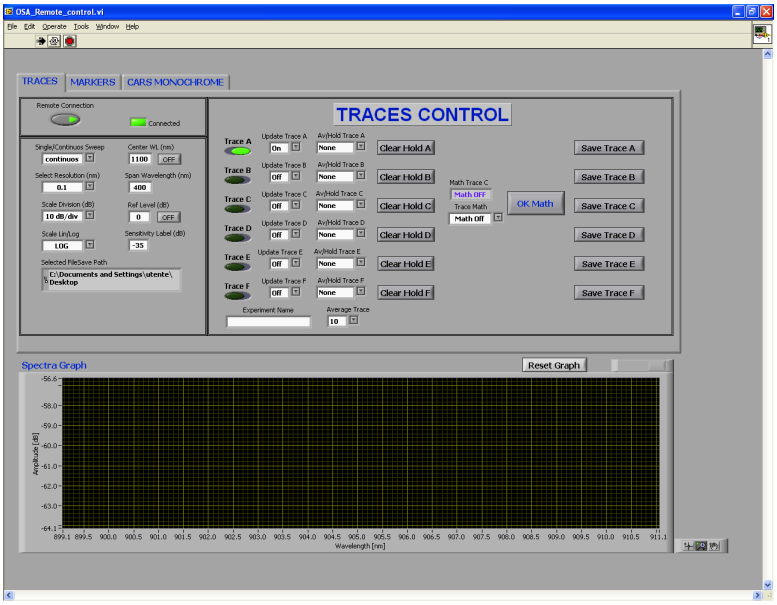

Fig. 3.6 Control interface of the optical spectrum analyzer based on Labview.

With this application was possible to control the main parameters of the OSA setting such as for example the spectral resolution, sensitivity, visualization of traces, mathematics between traces, etc.

The signal passing through the filtering block is analysed by means of a spectrometer (Avantes Avaspec2048) used as a detector block. In this way the whole spectrum of the radiation passing through the filter blocks is observed, collecting all the information about the relative strength of the residual excitation beams and generated CARS signal, together with any spurious signals that may appear. This capability is essential in order to design high-efficiency filtering blocks to isolate the CARS signal to be observed from any kind of optical disturbance.

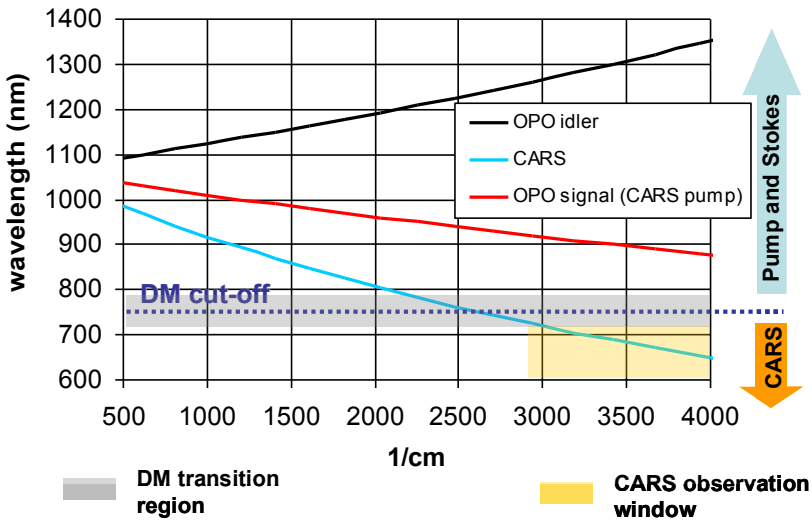

Fig. 3.7 Signal-idler excitation scheme: OPO signal as pump signal, idler as Stokes signal. Signal and idler wavelengths as a function of frequency detuning in cm^{-1}.

Efficient filtering of the excitation beams and of any other unwanted radiation is a crucial issue in CARS experiments, so that multiple filtering stages are to be used, tailored to the expected CARS wavelength (as shown in Fig. 3.3). This is particularly true for CARS microscopy applications, where the CARS signal to be

observed is very weak with respect to the excitation sources intensities. With this excitation scheme, where the CARS signal is particularly strong, the set-up of Fig. 3.3 filtering is not an issue, since the spectrometer performs as a tuneable narrow filter with very strong rejection. Non-critical filtering and automatic spatial and temporal overlap of the optical beams are the main reasons why signal-idler excitation scheme has been chosen for the first CARS experiments.

Signal-1064 Excitation scheme

With this excitation scheme the Stokes beam is provided by the 1064 output of the Nd:YVO_4 laser. The main advantage of this scheme is that 1064 nm is always the longest wavelength. This is an important point in view of the use of the confocal scanning microscope for CARS imaging purposes.

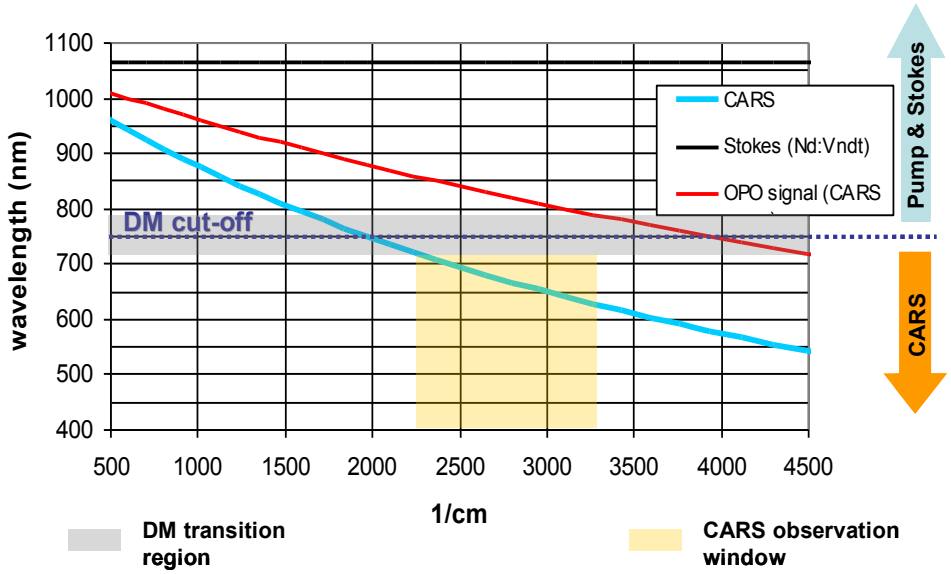

Fig. 3.8 Signal-1064 excitation scheme: OPO signal as pump signal, Nd:YVO4 output as Stokes signal (1064 nm). OPO signal wavelength as a function of frequency detuning in cm^{-1}.

The wavenumber region that can be reached using this scheme is shown in Fig. 3.8. As can be seen the generated CARS signal is placed more deeply in the visible, where the transmission of the dichroic mirror is optimal. On the other hand the pump wavelength gets nearer to the transition region of the dichroic mirror, so that observation is limited by the dichroic filter to the region from 2300 cm^{-1} to 3300 cm^{-1}, which is very well suited for the applications envisaged so far.

However by using this scheme the pump beam and the Stokes beam are generated separately and an optical delay line is necessary to superimpose temporally the pulses exiting the OPO and the Nd:YVO_4 laser. The delay line must also guarantee that the two beams, when combined, are collinear and spatially superimposed. The schematic of the experimental set-up that has been implemented is shown in Fig. 3.9.

As can be seen both outputs of the Nd:YVO_4 laser are used. The green output is sent as usual to the OPO to pump the non-linear crystal. The output at 1064 is sent through the optical delay line. The OPO configuration where signal and idler wave exit from separate ports is used in this excitation scheme. This is done simply by mounting a dichroic mirror inside the OPO which lets the idler wave go out through the main port and deviates the signal wave towards the other port. The idler wave is sent to a beam stop and blocked, whereas the signal wave is sent through a 1064 nm harmonic mirror where it is combined with the Nd:YVO_4 radiation providing the Stokes beam.

The combined beams are then sent to the launching optics. The launch and collection optics configuration is the one described above when discussing signal-idler excitation scheme.

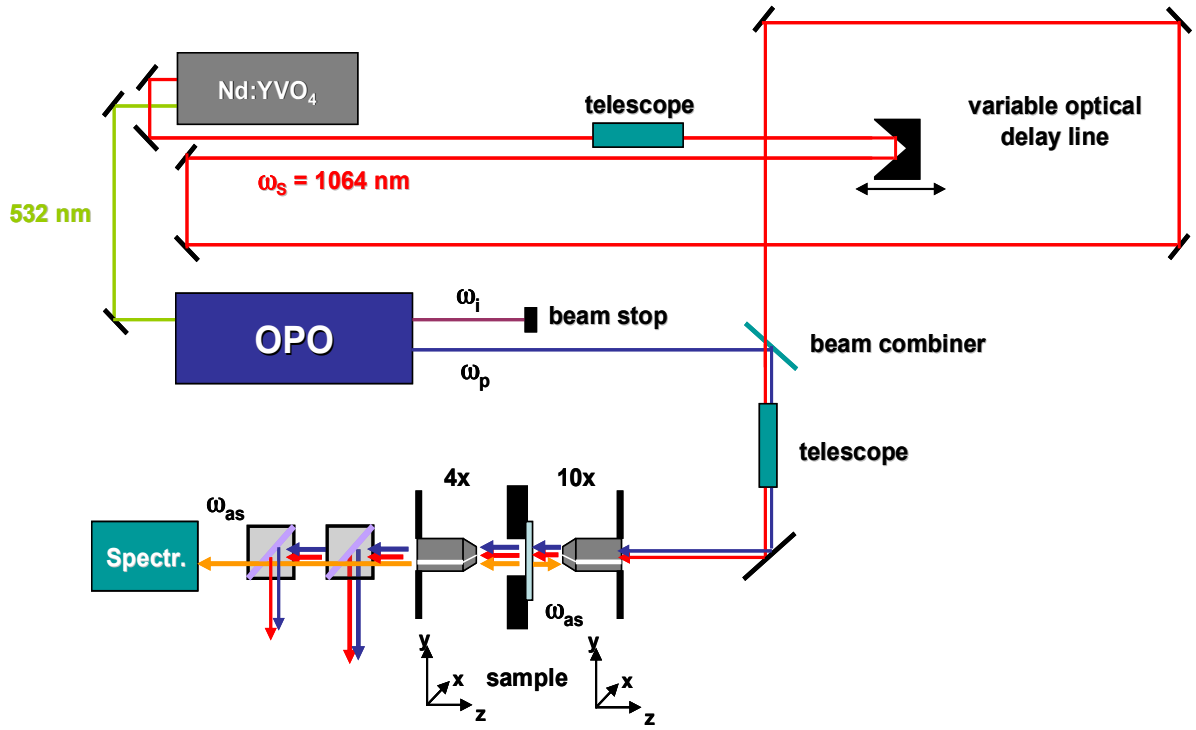

Fig. 3.9 Experimental set-up of the signal-1064 excitation scheme.

The signal passing through the filtering block is analysed by means of a spectrometer that is used as a detector block as in Signal-idler excitation scheme.

The main work in implementing Signal-1064 excitation scheme has been the design, trimming and tuning of the optical delay line. A folded geometry has been chosen because of the quite long delay necessary to synchronise the arrival of the pulses from the OPO and the pump laser (the OPO cavity is 4 m long). Since the OPO pulses are generated synchronously with the pump they must be combined with the 1064 pulses that gave origin to the generating 532 nm pump pulses in order to minimize strongly jitter. For this reason an accurate measurement of the relative delays of the pulse trains exiting the OPO and of the 1064 pulse train after the beam combiner resulted necessary.

A first approximate estimation of the delay line length has been done measuring the optical path of the pump pulses from the output port of the Nd:YVO_4 laser to the first mirror of the OPO cavity, the optical length of the cavity itself and then the length of the optical path from the output mirror of the OPO cavity to the beam combiner. The obtained gross estimation was around 5,5 m. The final geometrical layout of the delay line is shown in Fig. 3.6. The loop on the right has been devised to compensate for coarse mismatches in cavity length, whereas fine-tuning of the cavity is performed by means of a corner cube mounted on a precision translation stage with an elongation range of 2.5 cm. The total fine tuning correction range, 5 cm, corresponds in air to a time delay of about 170 ps. Picture of the full delay line is shown in Fig. 3.10.

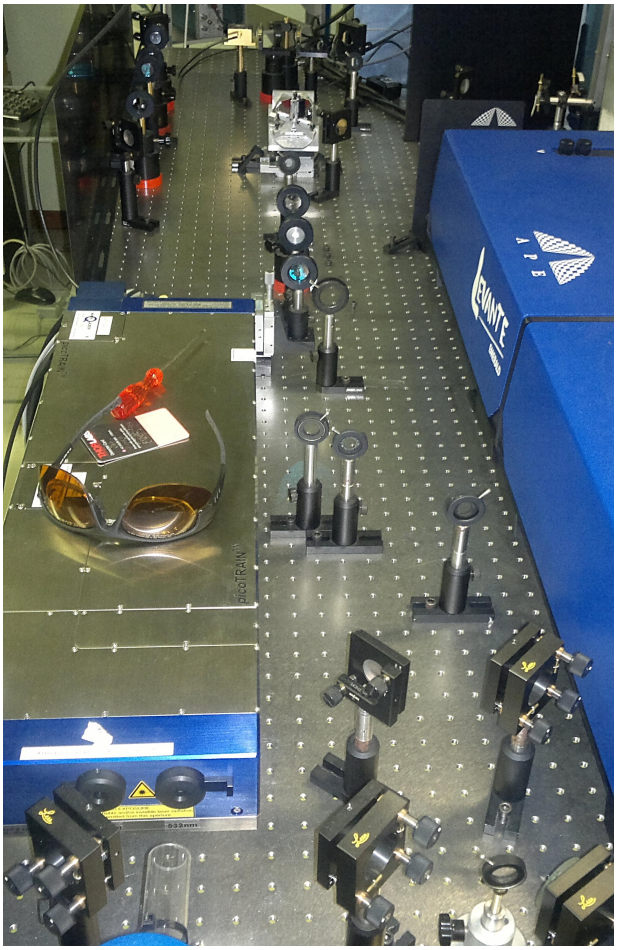

Fig. 3.10 Optical delay line realized for signal-1064 excitation scheme.

In order to tune the delay line, the actual delay between the pulses generated by the two sources is to be measured. To this aim the experimental configurations described below have been implemented.

For a coarse pulse delay measurement (on the order of nanoseconds) the pulses were detected with a fast photodiode (Thorlabs SV2-FC, Si, 300-1100 nm). The periodical electrical signal from the photodiode was sent to a sampling oscilloscope (Agilent MSO 6104A) in order to analyse the waveform. The bandwidth of the photodiode was 2 GHz (rise time 150 ps), whereas that of the oscilloscope was 1 GHz. The sampling oscilloscope was triggered using the electrical signal coming from the monitor photodiode mounted inside the Nd:YVO_4 laser. This signal consists of a train of electrical pulses at about 76 MHz, and is usually employed for real time measurement of the pulse repetition frequency of the laser. This setup allows an easy estimation of nanosecond time delays by measuring the temporal separation between the electrical pulse peaks on the traces generated by the OPO and by the Nd:YVO_4 laser. In this way gross tuning of the cavity has been made by changing the length of the looping section of the delay line to compensate for the measured time delay.

For fine-tuning of the delay line, in order to achieve good temporal overlap of the pulse trains, an optical autocorrelator was used. The autocorrelator, based on a scanning Michelson interferometer and a non-linear crystal, is part of the diagnostic equipment of the OPO (and pump laser) and is normally employed for real time measurements of the OPO pulse width. It can be equipped with a Silicon photodiode for the signal beams in the visible region, and a Germanium photodiode for the idler beam in the near infrared. For the alignment of the delay line the silicon photodiode was used. To compensate for the sensitivity non-

uniformity of the autocorrelator photodetector the signal wave was attenuated so as to detect pulses of amplitude comparable with that of the 1064 nm beam.

When the pulse delay is less than the measurement window of the autocorrelator (100 ps), two distinct pulses can be observed that can be readily superimposed acting on the precision translation stage that moves the corner cube.

Spatial overlap of the excitation beams at the beam combiner is another important issue. The full length of the delay line from the Nd:YVO_4 output port to the beam combiner is about 6 m as resulted from delay measurements and fine temporal tuning. Over such a distance the spot size of the 1064 nm beam resulted too large due to beam divergence. In order to mitigate this problem some telescopes have been placed along the delay line path. A telescope can in principle correct for beam divergence and act as a collimator. A single telescope module hardly could set to fully compensate the beam divergence. Further reduction of the spot-size has been achieved adding a further telescope and by means of spatial filters (iris diaphragms). Spatial filtering however is not optimal, since it does introduce additional loss and diffraction effects.

Mutual alignment of the excitation beams has been achieved controlling the beam height step by step along the delay line by means of a series of iris diaphragms and by using mirror steering mounts, used to align and superimpose the 1064 nm beam to the OPO signal beam on the combiner in front of the OPO exit port (see fig. 3.9). The total loss of the delay line was about 10 dB.

Initial practical realization of the two excitation schemes and preliminary results

Signal-idler excitation scheme

Preliminary results were obtained using the experimental set-up of Fig. 3.3 with the optical bench composed by a 10x focusing objective (UPLSAPO 10x NA=0.4, Olympus), the sample and a 4x collector objective (UPLSAPO 4x NA=0.16, Olympus). The signal collected from the sample was isolated from input incident laser pulses by means a dichroic mirror, sent on a fiber collimator and measured through a spectrometer (Avaspec2048, Avantes). Pictures of the actual experimental configuration are shown in Fig. 3.11.

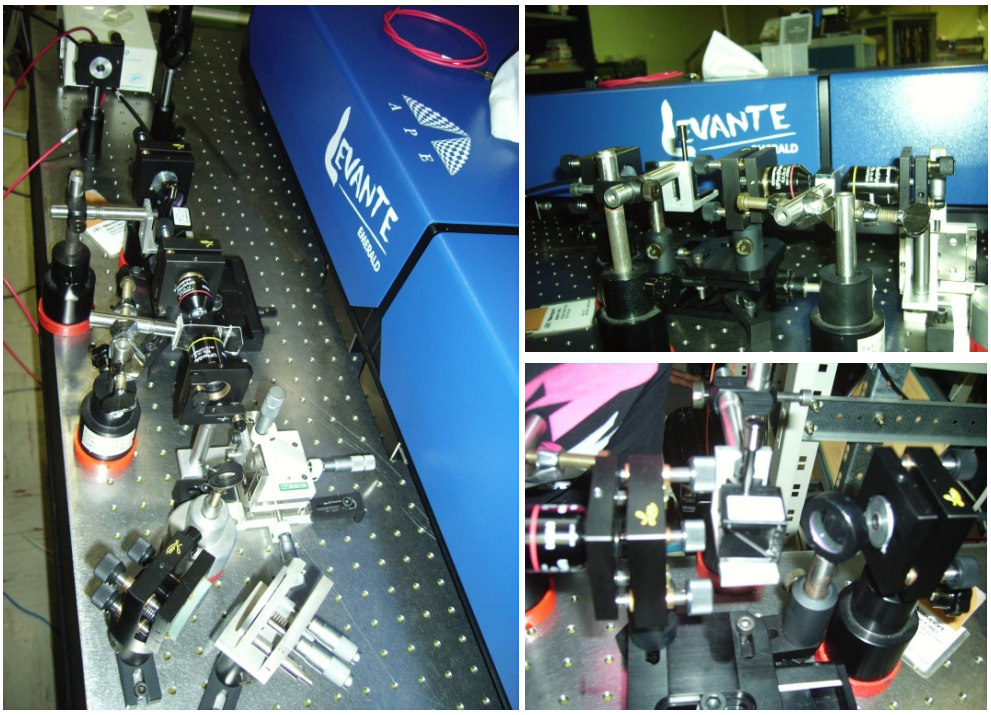

Fig. 3.11 Picture of the focusing and collection optics (left and upper right), filtering block and fiber collimator (lower right).

Spectral data were recorded in forward direction varying signal-idler wavelengths, in order to characterize the polystyrene plate sample in the range between about 2700-3150 cm^{-1} with a resolution step of about 5 cm^{-1}. This step corresponds roughly to the spectral resolution deriving from the used pulse widths (about 6 ps).

The expected CARS spectrum in the wavenumber region of interest was calculated numerically from the measured spectrum using a specifically made routine written in Matlab. As discussed in the previous chapter, the CARS spectrum of a material does not overlap exactly to the spontaneous Raman spectrum because the CARS signal has the following dependence on the third order susceptivity $\chi^{(3)}$ of the material:

$$\left|\chi^{(3)}_{CARS}\right|^2 = \left|\chi^{(3)}_{NR} + \Re\left(\chi^{(3)}_R\right) + i\Im(\chi^{(3)}_R)\right|^2 \qquad (25)$$

In order to calculate the CARS spectrum, the measured Raman peaks were fit to Lorentzian curves and the real and imaginary parts of the complex susceptibility were extrapolated for each transition. All the computed susceptibilities were added up to give the total resonant contribution to $\chi^{(3)}$. As a first

approximation, the non-resonant contribution $\chi_{NR}^{(3)}$ was assumed constant and equals to one. The CARS spectrum of the polystyrene sample was then computed using Eq. (25). The final result is shown in Fig. 3.12.

The experimental CARS spectrum was obtained measuring in several steps the signal coming from the sample. For each step the wavelength separation (in cm^{-1}) is tuned to the desired value by changing the signal-idler wavelengths; the typical step is around 10 cm^{-1}. Then the whole optical spectrum is collected. An example of a typical spectrum observed in our CARS experiments is shown in Fig 3.13, where the CARS signal (middle) is clearly seen together with the residual OPO signal (right) and a spurious signal (right) that can be identified as the second harmonic of the idler wave. These steps are repeated until the whole measurement spectral region is completely scanned. The CARS signal peak level for each wavenumber detuning is extracted from the whole measured spectrum by means of a specific C++ script made to the purpose. The CARS spectrum was then obtained normalizing CARS signals taking into account incident pulses power.

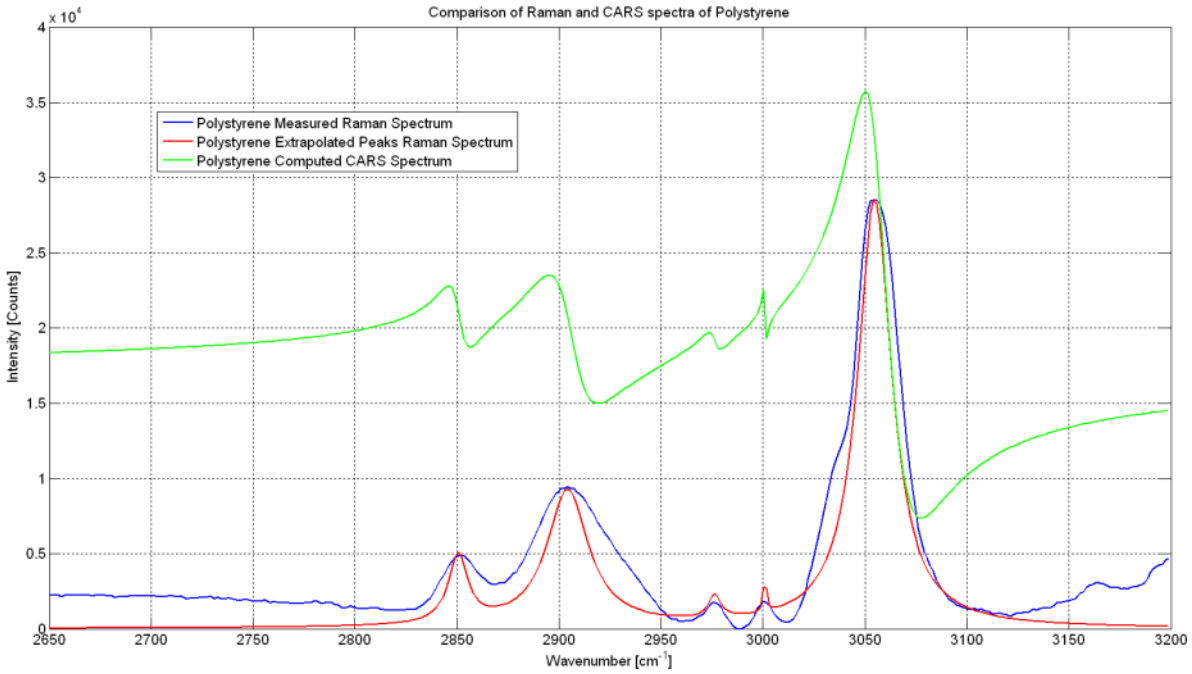

Fig. 3.12 Measured Raman Spectrum (blue curve), extrapolated Raman spectrum (red curve), calculated CARS spectrum (Green Curve).

In signal-idler excitation scheme the total power exiting the OPO can be fully exploited. Typically in the experiments described below the total power measured before the focussing objective exceeded 1 W. The signal average power (CARS pump beam) is about 550 mW, whereas that of the idler (Stokes beam) is about 680 mW, with an average total power of about 1.2 W.

With such powerful excitation beams a quite strong CARS signal is expected as soon as the sample is brought into focus, as can be seen in Fig. 3.13.

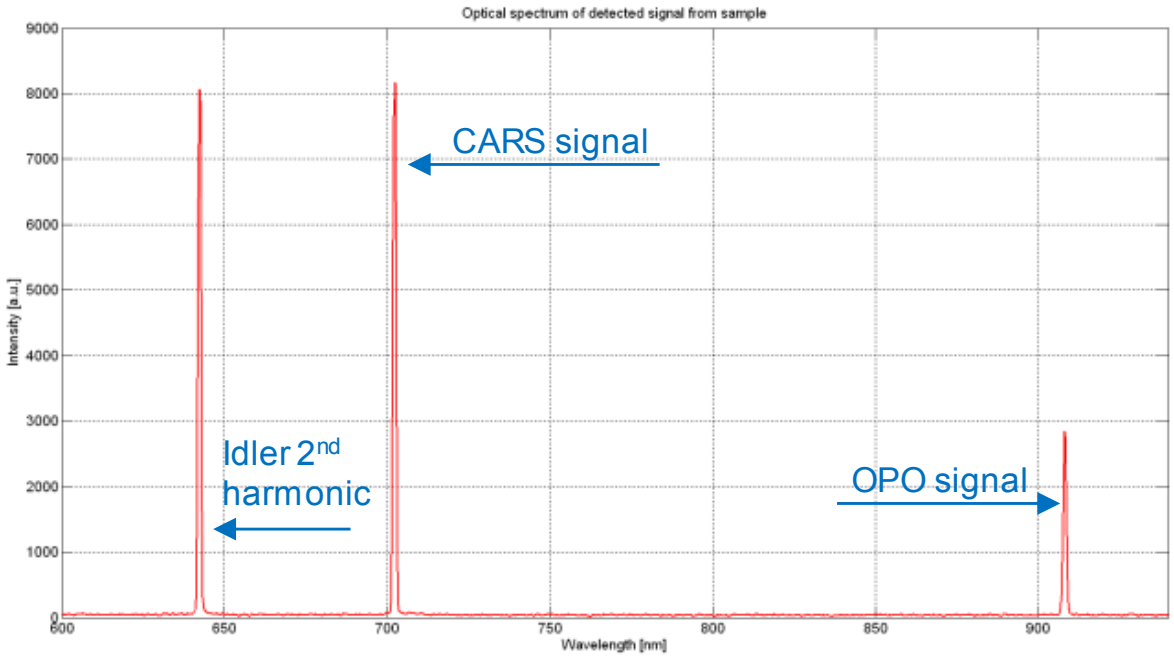

Fig. 3.13 Example of a spectrum measured out of the polystyrene sample.

The dependence of the CARS signal intensity on the incident laser pulses power was estimated collecting several spectra taken varying the power of the OPO signal. The data obtained from the measurements are presented in Fig. 3.14. As can be seen, the obtained curve is in agreement with the theoretical model [see Eq. (9)] whereby a cubic dependence of the CARS signal on the power of the OPO signal is predicted. This is a further confirmation that the observed signal is actually generated by CARS.

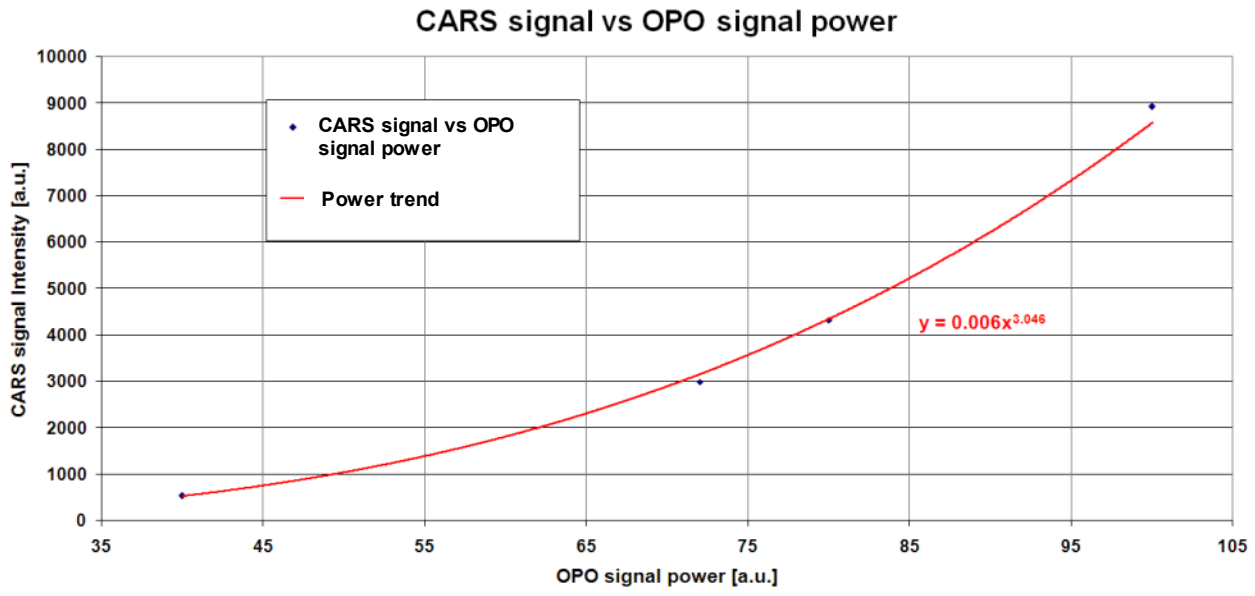

Fig. 3.14 Measured dependence of the CARS signal on the OPO signal power.

Strong CARS signals are clearly observed whenever the signal-idler wavelengths are tuned to a resonant vibrational transition of polystyrene (see Fig. 3.15). The scan was carried out with a 10 cm^{-1} step in the 2900-3200 cm^{-1} spectral region. In terms of wavelength the OPO signal is scanned over a window of 11 nm. Over such moderate scanning intervals tuning can be done simply changing the angle of the birefringent filter inside the OPO cavity using the OPO controller.

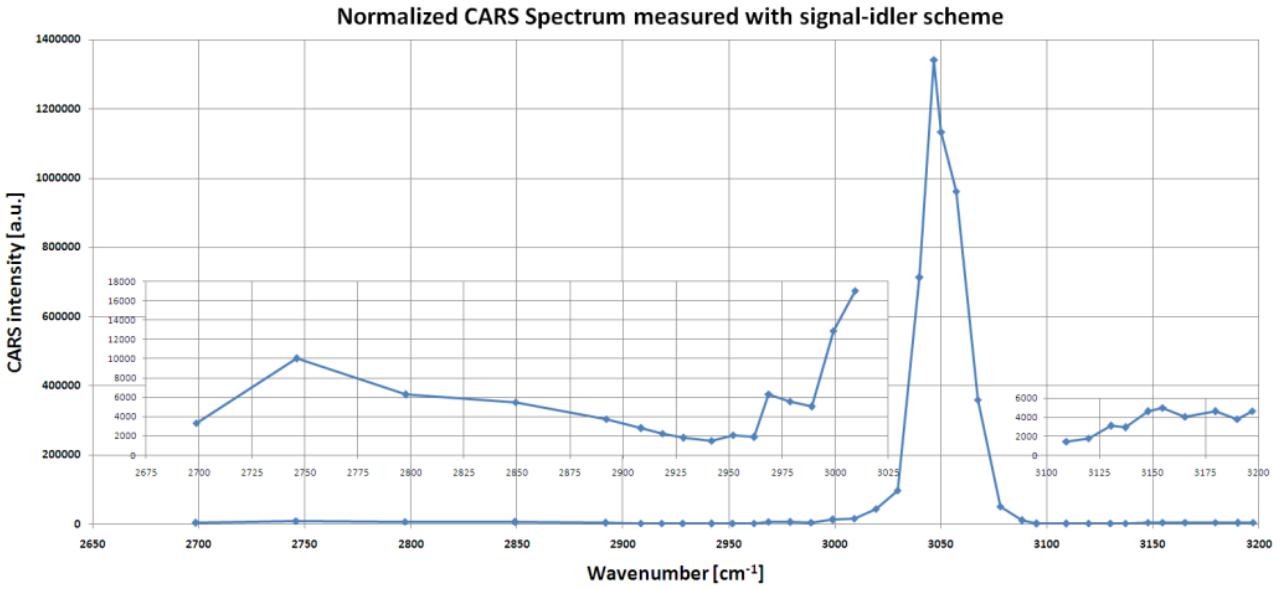

Fig. 3.15 Measured CARS spectrum with signal-idler excitation scheme.

A much larger step (about 50 cm^{-1}) was used on the 2700-2900 cm^{-1} range, which required also to change the non-linear crystal temperature to tune properly the OPO. When excitation wavelengths are tuned off-resonance the CARS signal decreases accordingly and the contribution of the non-resonant background appears, according to the CARS theoretical model, see Eqs. (9), (12) and (25), as can be seen in the insets of Fig. 3.15. The characteristic minimum of emission after the peak (see Fig. 2.2) is clearly visible in the inset on the right. The peak appears around 3050 cm^{-1} as expected.

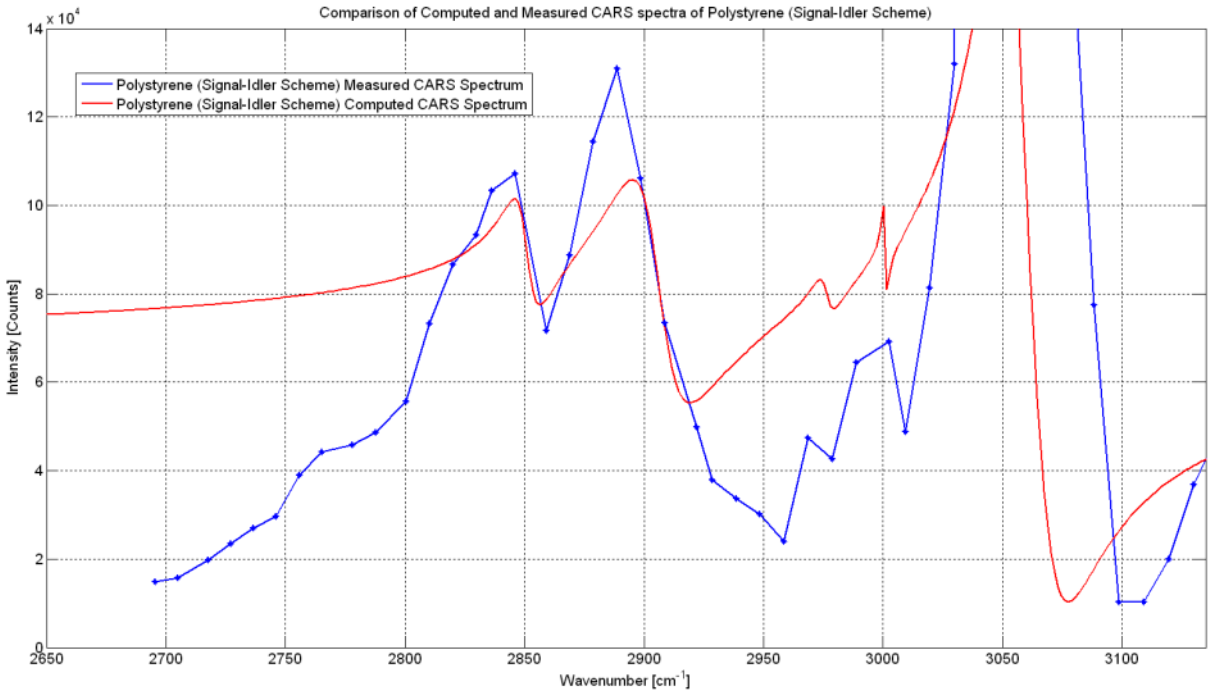

Fig. 3.16 Measured CARS spectrum with signal-idler excitation scheme with higher resolution (blue curve). Calculated CARS spectrum given for comparison (red curve).

In order to obtain more information about the spectral peaks around the main peak at about 3050 cm^{-1}, a second set of CARS measurements was carried out further optimizing the optical alignment of the system,

letting saturate the spectrometer response around the main peak at about 3050 cm^{-1}. The aim of this measurement was to verify a correspondence between the computed and the measured CARS spectrum. In this measurement a longer integration time was set on the spectrometer and the number of measurement steps was increased (step width is around 10 cm^{-1}).

The result of the measurement is shown in Fig. 3.16 (blue line). The scan window covers a wavenumber interval larger than 400 cm^{-1} with 50 sampling points. The total scanned OPO signal wavelength window is slightly more than 20 nm. As can be seen the obtained curve is consistent with the computed CARS spectrum (red line). All the expected peaks have been observed in the CARS measurement. There are however slight differences that can be ascribed to the fact that the computed spectra are approximated (not all the peaks were taken into account and a constant non-resonant background on the overall spectral window of observation was assumed) and that, during the scan, the OPO signal shows amplitude and wavelength instabilities that are affecting the result of the measurement. Approximately the wavelength fluctuation of the OPO signal observed during the measurement time (typically about 30 s per point on the charts) is of the order of ± 0.1 nm, whereas power fluctuation is of the order of ± 5%.

Signal-1064 excitation scheme

A CARS characterization experiment using the same polystyrene sample as reference material was also carried out using as excitation radiation, the combination of the OPO signal and the 1064 nm output beam of the Nd:YVO_4 laser.

As previously described, the two beams were overlapped in space and in time using a delay line and the resulting beam was sent to the same optical set-up used with Signal-idler excitation scheme (see Fig. 3.11).

The polystyrene plate sample was characterized again in the range 2700-3100 cm^{-1} with a resolution step of about 5 cm^{-1}, following the same procedure as described previously when discussing the measurements with Signal-idler excitation scheme.

OPO signal wavelength has been scanned in the region around 803 nm. The corresponding idler wavelength (not used) scans the region around 1576.4 nm. The wavenumber difference between the two is about 6110 cm^{-1}, two times the wavenumber difference between signal wavelength and 1064 nm. This is because in this scheme the Stokes frequency, ω_S, is half the frequency of the OPO pump, ω_{pOPO}. Thanks to this property, a given change in terms of cm^{-1} is obtained by varying the signal wavelength with a step that is two times that needed with signal-idler excitation scheme. The expected CARS signal is around 645 nm.

With this excitation scheme the total power impinging on the focussing objective was typically about 300 mW, of which about 200 mW of OPO signal (pump wave) and about 100 mW of 1064 nm (Stokes signal).

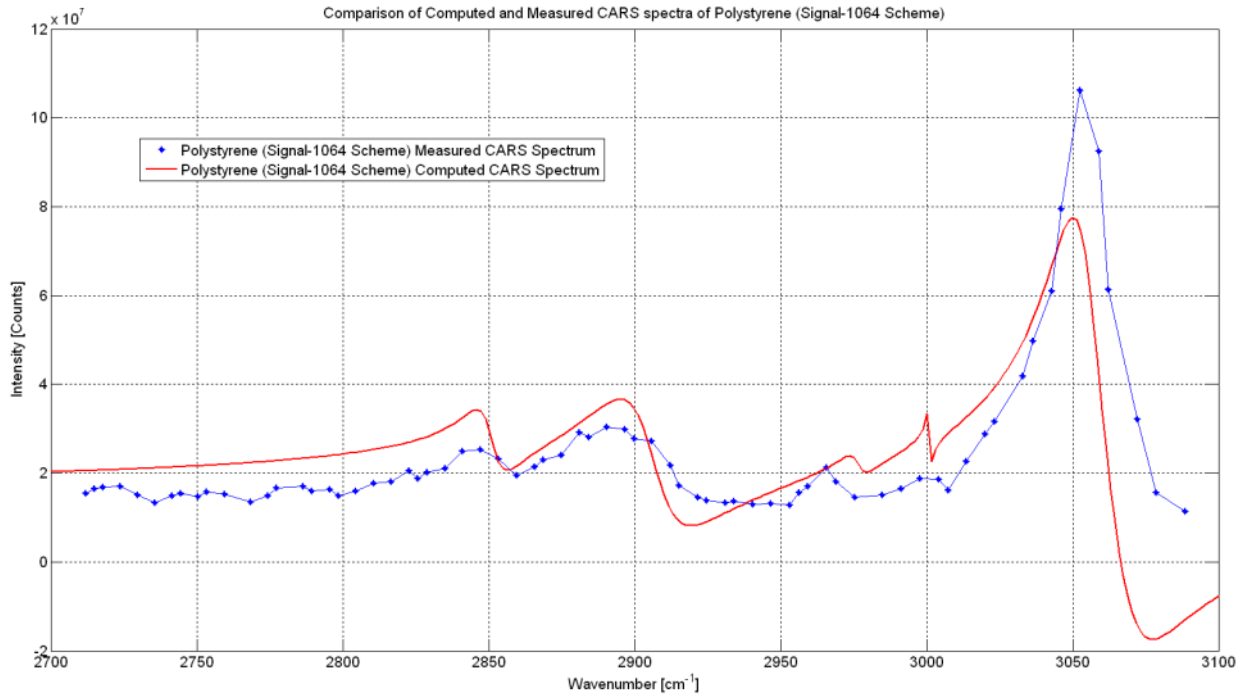

Fig. 3.17 CARS spectrum measured with signal-1064 excitation scheme (blue curve). Expected behaviour of the CARS intensity is also shown for reference (red line).

Also in this case strong CARS peaks were clearly visible when the OPO was tuned to a resonant vibrational transition of polystyrene. When source wavelengths were tuned off-resonance, CARS signal decreased accordingly and non-resonant background appeared.

The obtained CARS spectrum is shown in Fig. 3.17 (blue curve). The scan window covers a wavenumber region of about 400 cm^{-1}, with 68 sampling points. In terms of wavelength this corresponds to a scan window of about 27 nm. Over such a wide wavelength range, the tuning of the OPO, done manually, required to change several times the temperature of the NL crystal and was quite laborious. Moreover, attention has been paid to maintain the OPO power as constant as possible during the wavelength scan. In order to do this at each wavelength step the cavity length had to be slightly adjusted. In order to maintain a given power level the cavity was slightly detuned when the power was above the target level or better tuned when too low.

The measured spectrum, as can be seen from the figure, is consistent with the (simplified) computed CARS spectrum (red curve). All the expected peaks can be identified in the CARS measurement. The deviations can be ascribed to the same reasons previously mentioned in the discussion of the results obtained with Signal-idler excitation scheme. However, the uncertainty on the experimental points in Fig. 3.17 is expected to be less than in previous measurements, since a smaller error in the normalisation procedure is expected by keeping the power constant during the scan.

Filtering issues for CARS imaging

In CARS microscopy, like in confocal fluorescence microscopy techniques, isolation of the expected signal from all signals coming from the sample is a very important issue. In fact, the CARS signal is typically orders of magnitude weaker than the excitation signals, so it is necessary to ensure that only the CARS signal arrives on the detector with all other disturbances effectively suppressed.

A commercial microscope (BX51WI, Olympus) equipped with a confocal scan head (FV300, Olympus) have been chosen to realize multimodal CARS-SHG-TPEF microscopy techniques at the I.N.Ri.M. laboratories.

In the confocal microscope scan head is installed a standard filter set for fluorescence microscopy, not suited to perform the strong suppression of the excitation signals before the PMT at the wavelengths needed for CARS microscopy experiments. Consequently, at the beginning CARS imaging could not be performed, even using Signal-1064 excitation scheme with which the overall optical system performs much better.

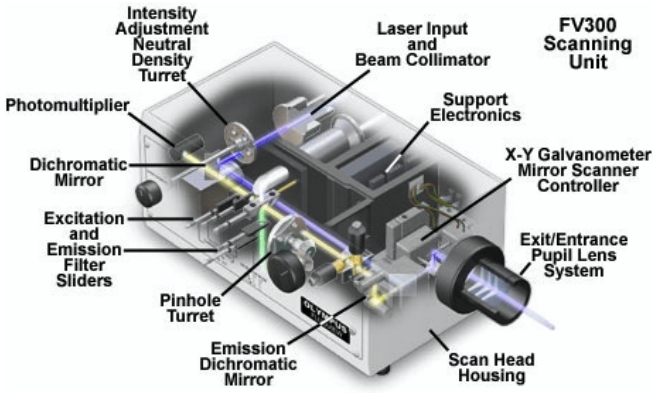

Fig. 3.18 Olympus FV300 scanning unit with main components highlighted.

This fact has been verified by performing a CARS spectroscopy experiment on the polystyrene sample using signal-1064 excitation scheme in the experimental conditions used for sample imaging in epi-detection. In this experiment the OPO signal beam and the 1064 nm beam are launched into the confocal microscope and focused on the sample. The generated CARS signal is collected backwards by the focussing optics, passes through the microscope again, is let trough by the dichroic mirror and goes to the scan unit PMT. The electrical output of the PMT is measured directly by means of a digital multimeter (Agilent 34401A).

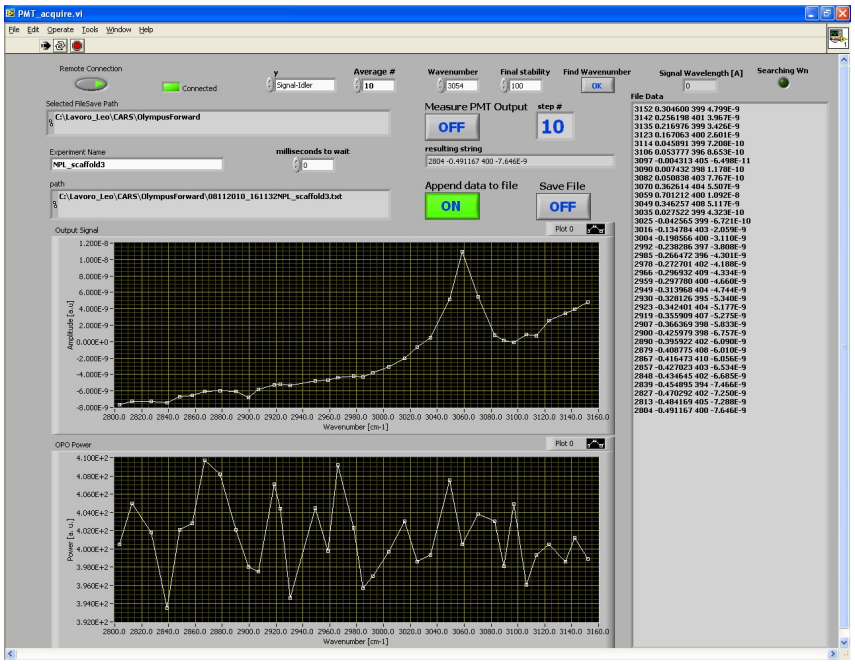

Fig. 3.19 Graphic interface of the control software developed to measure CARS spectra through the acquisition of the output PMT voltage.

The result, shown in Fig. 3.20 (blue curve), clearly indicates that the measurement does not fit with the expected CARS spectrum (red curve) and that most of the radiation measured by the PMT is spurious signal. In particular we observed that the measured signal at the PMT output is strictly correlated to the OPO signal power variation with wavelength and not to the CARS signal. In fact, the dichroic mirror inside the scanning head (the same used for the previously described forward CARS experiments) does not reflect away all the power of the excitation beams.

Thus, the small portion of the OPO signals reflected from the sample, still bigger than the expected CARS signal, is transmitted through the dichroic filter and reaches the PMT where overwhelms the CARS signal (it is important to note that with signal-1064 excitation scheme the OPO signal sits at a wavelength that can be detected very well by the PMT).

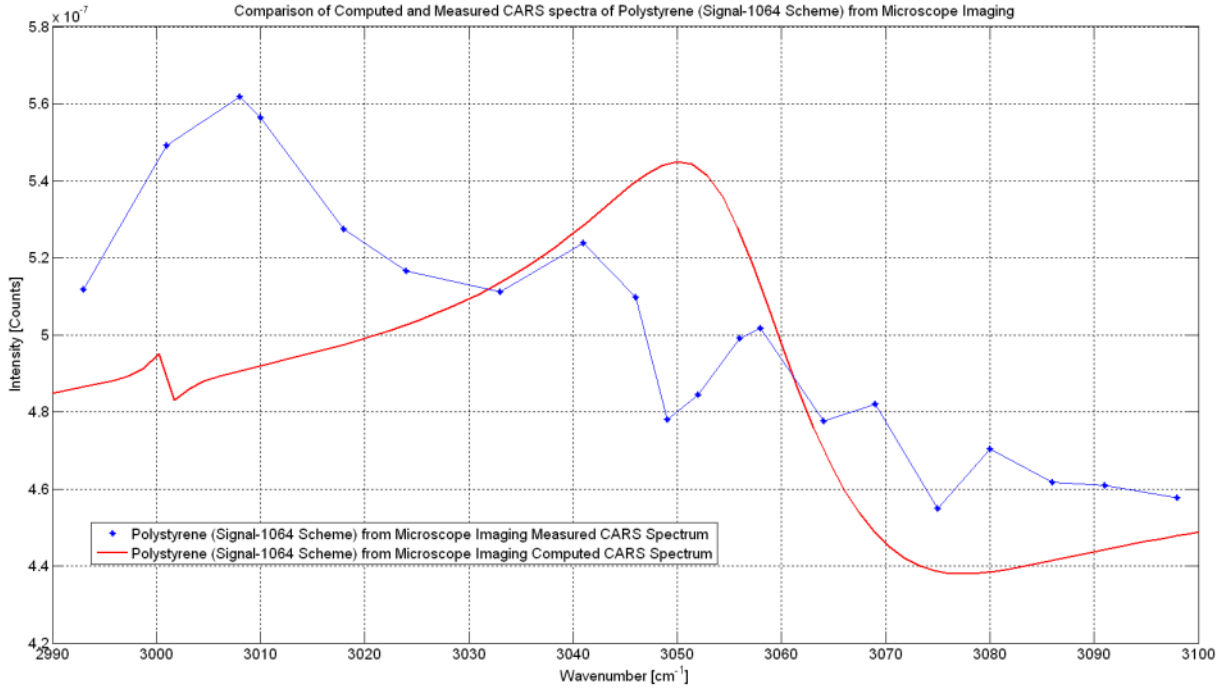

Fig. 3.20 Signal in the CARS band measured by means of the confocal microscope PMT. Expected behaviour of the CARS intensity is also shown for reference (red line).

Fig. 3.21 shows the recorded spectrum when the dichroic mirror DM740 is used as the only filtering stage between the 4x collector objective (UPLSAPO 4x NA=0.16, Olympus) and the collimator lens. As can be seen, very strong unwanted signals appear in the region between 640-850 nm. These signals correspond to the suppressed side modes of the OPO signal and to the OPO signal line itself. As can be seen other spurious lines also appear than can be ascribed to the 1064 nm laser and to harmonics of the OPO idler.

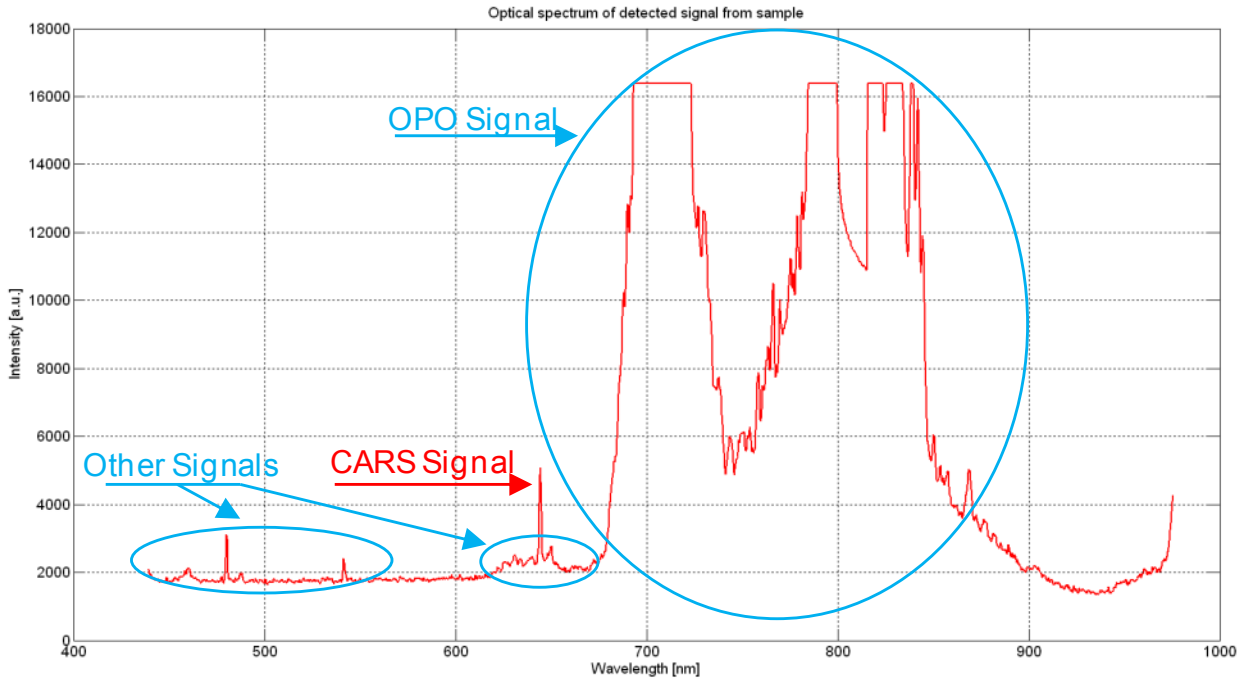

Fig. 3.21 Spectrum of the forward light passing through the dichroic mirror after CARS interaction. As can be seen the CARS signal is merged in a sea of disturbances.

As can be inferred from Fig. 3.22, the strong side mode of the OPO signal around 700 nm can pass through the dichroic mirror almost undisturbed.

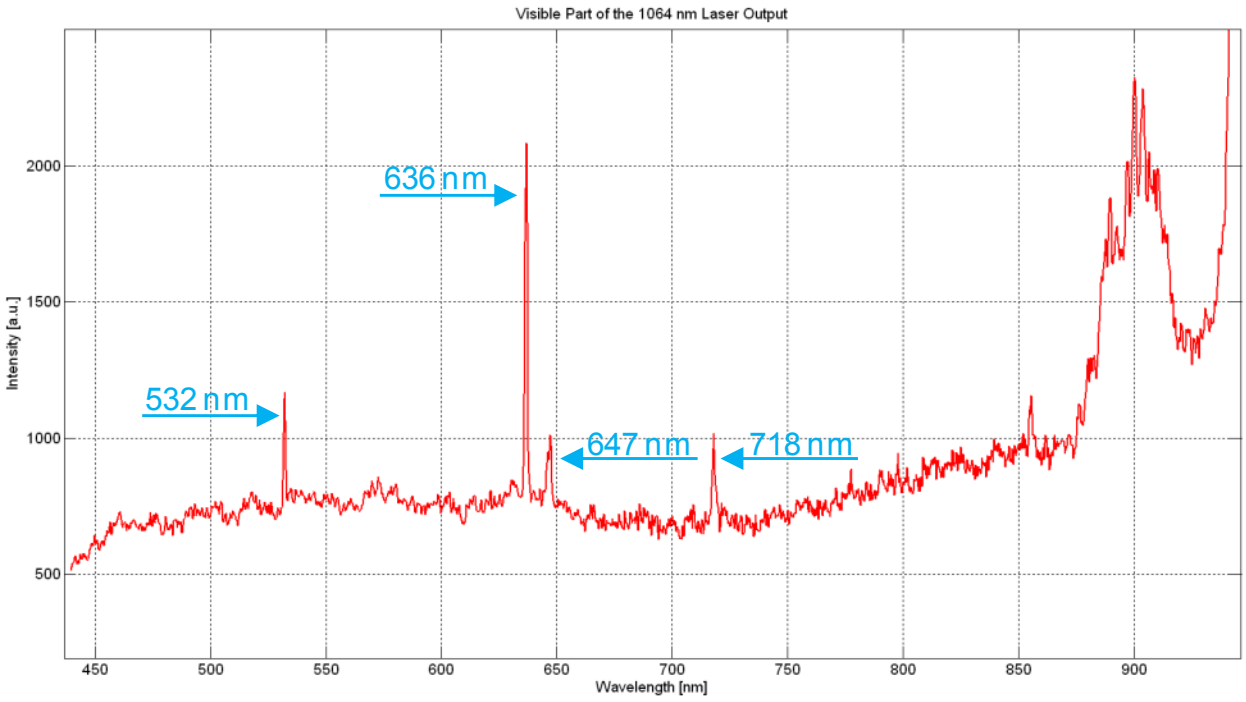

Fig. 3.22 Measured Spectrum of the Nd:YVO_4 laser.

In order to identify all the spurious signals appearing in the CARS spectrum, the spectrum of the 1064 laser has been measured in the region of interest. The result is shown in Fig. 4.18. As can be seen a series of lines do appear at wavelengths very close to the CARS signals to be observed.

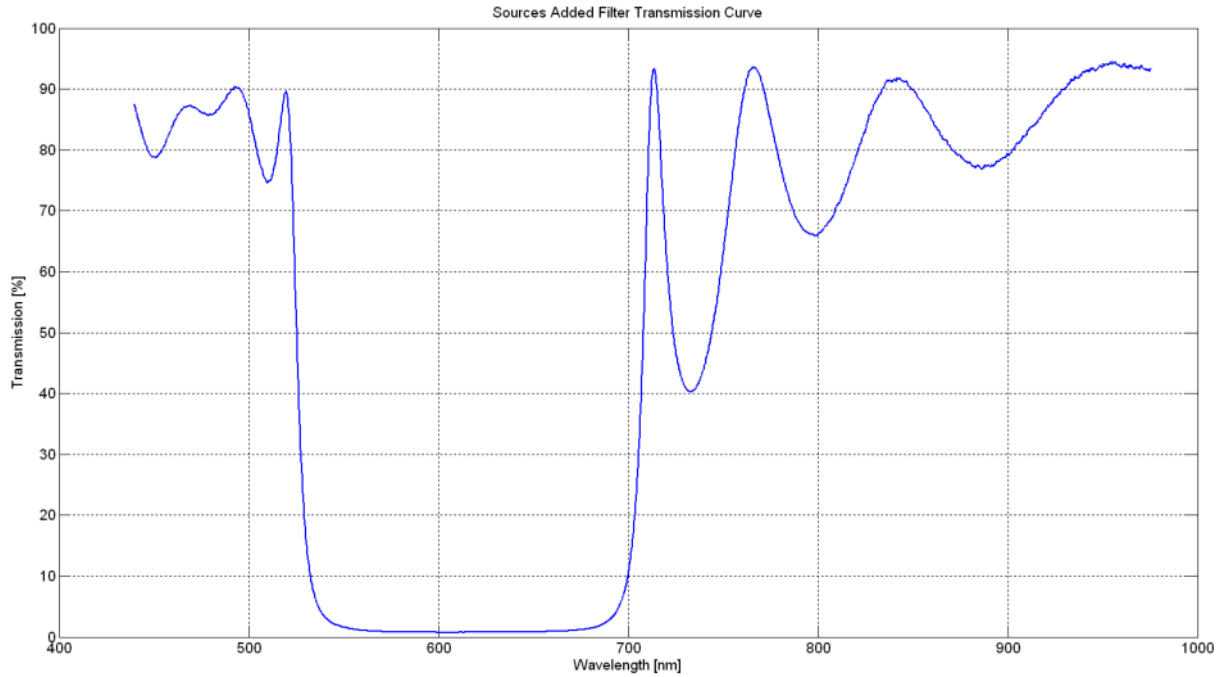

Fig. 3.23 Measured spectral transmittivity of the dichroic mirrors used to clean the signal line of the OPO.

Consequently, it is very important to clean out accurately unwanted features of the excitation beams and use very strongly selective filtering in front of the detector. To this aim, we looked for additional filters among the optical components available in the lab. Suitable filters were finally selected after optical characterization by means of the set-up shown in the inset of Fig. 3.4.

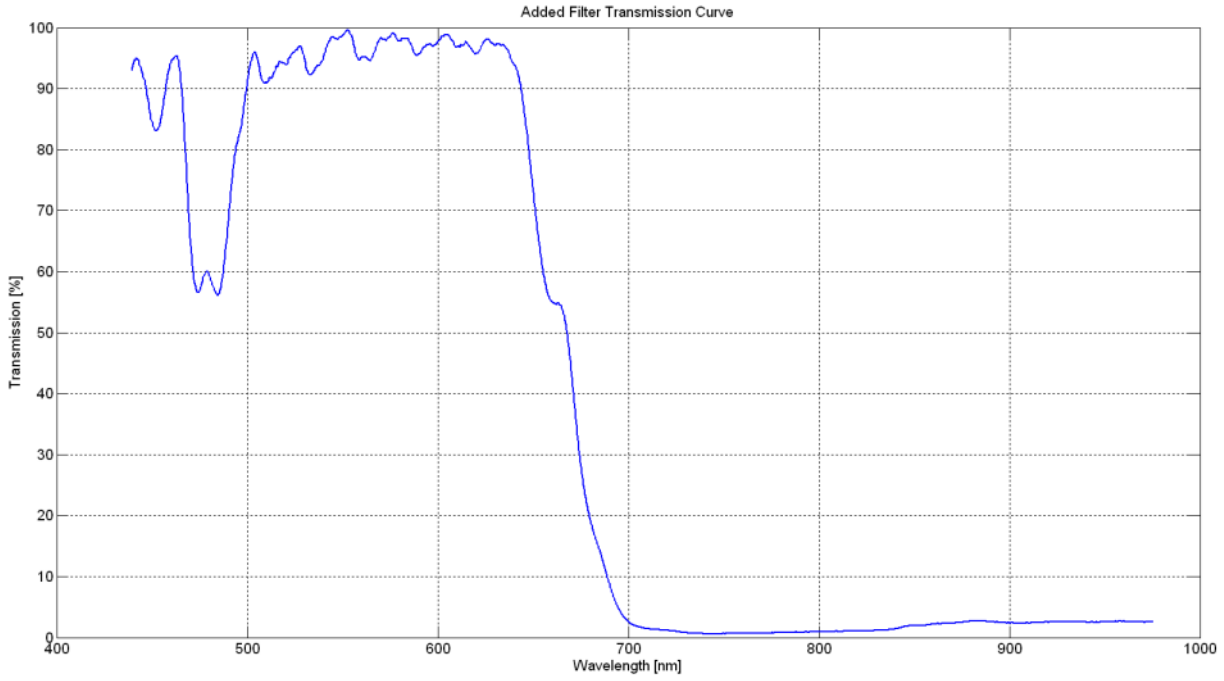

Fig. 3.24 Measured spectral transmittivity of the cascaded short pass filters used to reject the residual OPO signal light.

The spectral transmission curves of the selected filters are shown in Fig. 3.23 and 3.24. Figure 3.23 shows the transmission characteristics of a dichroic mirror designed to selectively reflect radiation from a red laser. It has been used to clean the unwanted signal features in the spectral region where CARS is expected. The filter is placed before the focusing objective. Fig. 3.24 shows the transmission characteristics of two cascaded short pass filters, used to clean out the residual OPO signal before detection.

When these additional filters are inserted, the observed spectrum is considerably improved, as can be seen in Fig. 3.25. In particular, a much better suppression of unwanted signals is apparent and a considerable reduction of stray light is observed (the baseline is lower than in Fig. 3.21). This notwithstanding, the residual OPO signal power is still much stronger than the CARS signal. If a signal like this arrives at the PMT of the confocal scan-head, the OPO signal beam mainly generates the measured PMT current. This corroborates the interpretation of the results shown in Fig. 3.20. Therefore, the whole filtering chain, as it is now, is insufficient to perform reliable CARS imaging with signal-1064 excitation scheme. Stronger filters, very well-tailored to the spectral characteristics of the signal to be observed, are thus required.

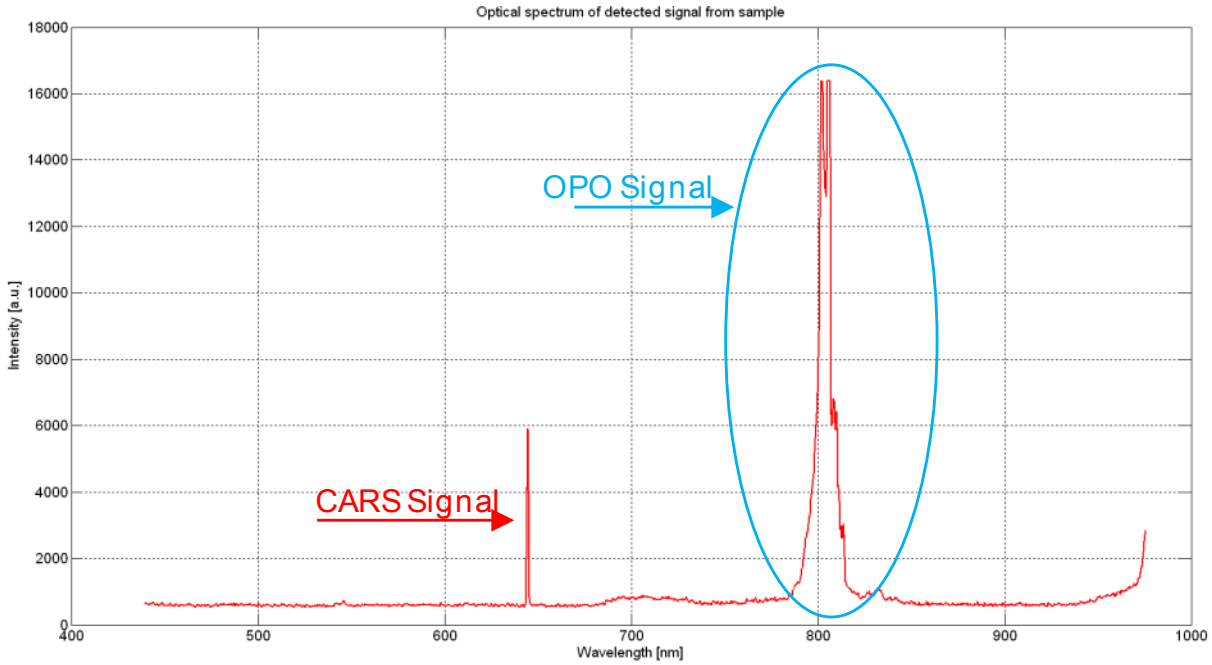

Fig. 3.25 Observed spectrum at the detector with improved filtering and OPO signal cleaning.

Using the improved filter block a forward CARS experiment was then carried out through the confocal microscope system. On the basis of the results of Fig. 3.17, a silver mirror replaced the dichroic mirror in the confocal scanning head excluding epi-detection.

The signal-idler excitation scheme was used to excite the sample. The total power at the input of the scanning head was 1.15 W (idler 700 mW, signal 450 mW), whereas that measured on the sample (below the focusing objective) was 110 mW (signal 70 mW, idler 40 mW).

Again, the wavenumber region around 3000 cm^{-1} was scanned with the usual measurement procedure. The scan step was about 10 cm^{-1}.

The result is shown in Fig. 3.26. The agreement with the predicted spectrum (red line) is quite good. All the relevant features do appear despite the fact that the received signal is much lower than in the previous measurements. It must be kept in mind, however, that this experimental configuration is clearly not meant for CARS spectroscopy. In CARS imaging experiments the excitation source is tuned to the emission peak of the chemical species to be observed and the sample is scanned to identify the regions were the species under study is present.

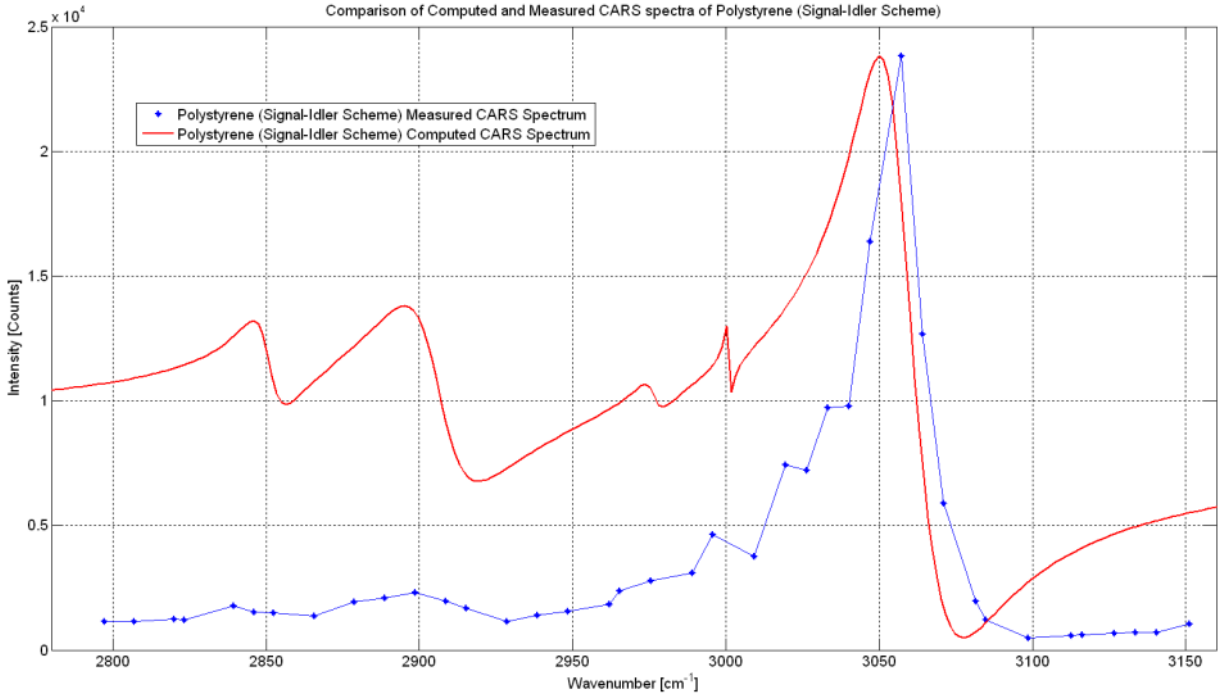

Fig. 3.26 CARS spectrum measured using Olympus microscope in forward detection.

This experiment has been carried out to demonstrate that using our equipment for confocal microscopy a CARS signal can be generated and sufficiently well isolated from disturbing signals so as to guarantee unambiguous detection.

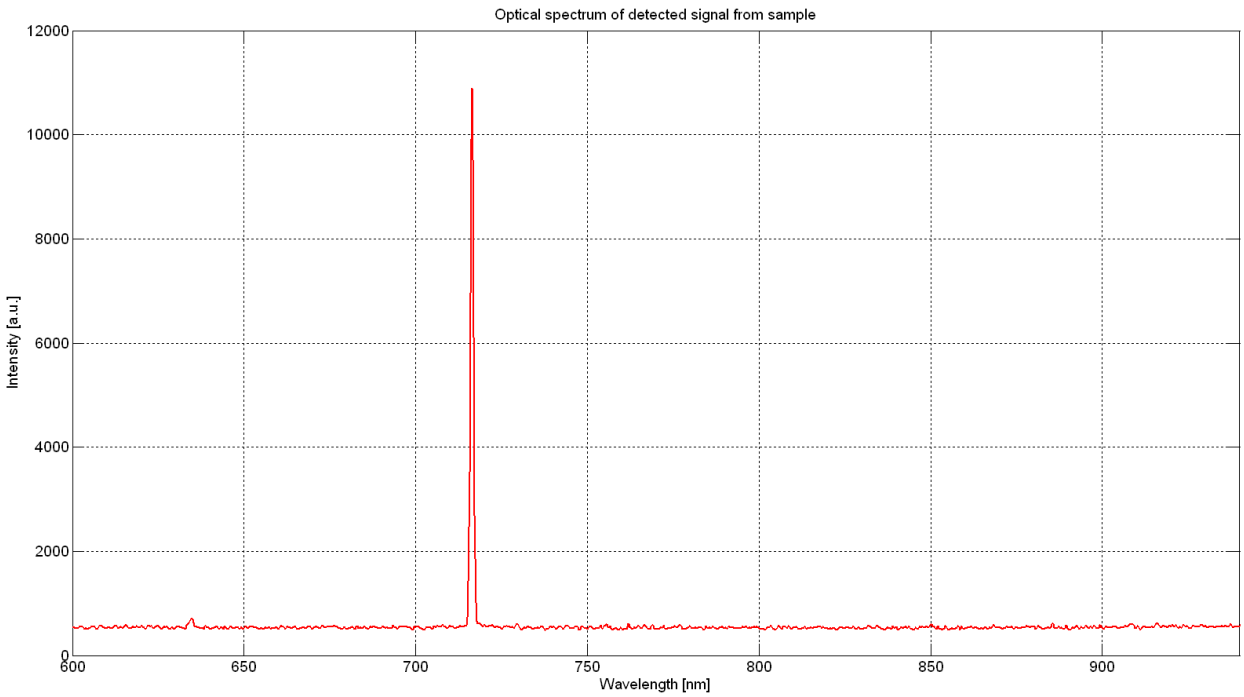

Fig. 3.27 Measured output spectrum after filtering. The CARS signal is the only strong feature, all disturbances have been efficiently suppressed.

The good performance of the filtering block (dichroic mirror plus short pass filters at the receiver, cleaning filter on the OPO signal) is demonstrated in Fig. 3.27 where the CARS spectrum at around 3030 cm^{-1} is shown as recorded by the spectrometer (integration time 300 ms).

The better suppression of the excitation beam is due to the fact that with signal-idler excitation scheme the wavelength of CARS signal is farther from that of the excitation beam and that the dichroic mirror at 915.6 nm is more efficient than in Fig. 3.25.

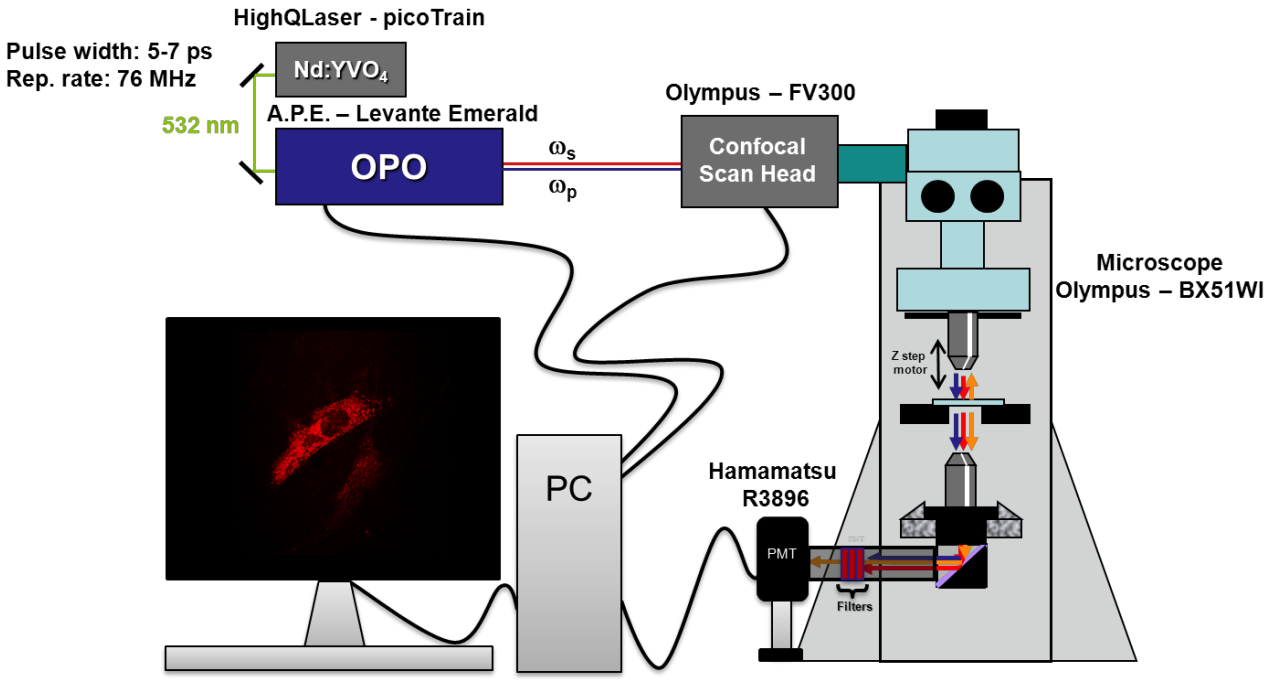

Fig. 3.28 Schematic of the CARS microscopy setup.

A PMT (model R3896, Hamamatsu) was acquired and used as detector in forward direction. A custom made holder for the PMT and the optical filters was designed and realized to protect the optical path from stray light disturbances. The holder allows changing easily the filter configuration thanks to five interchangeable filter holders and embeds also a plano-convex lens (with focal length f=25 mm) used to make the scanning beam fit the active area. One of the most important issues in multimodal microscopy is in fact to filter the contrast signal from the excitation sources and other signals that can be excited on the sample. Two types of filter were used for this purpose, shortpass filters to block excitation sources that have longer wavelengths than the generated nonlinear signals, and bandpass filters for further selective discrimination of the interested spectral window.

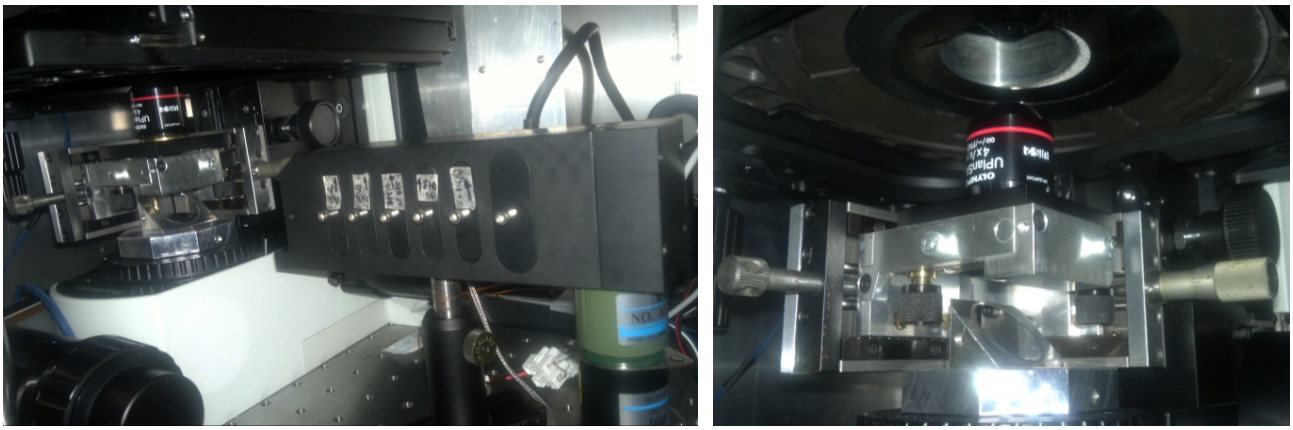

Fig. 3.29 Optical setup for forward CARS detection. Filter and PMT holder designed and realized at INRIM (left). Objective holder with all the degrees of freedom designed and realized at INRIM.

A custom-made objective lens holder with four degrees of movement (the three directional axis and tilting angle) to allow forward detection was designed and realized (Fig. 3.29).

There are two main interesting spectral regions for CARS spectroscopy, that are the “fingerprint region” from about 500 to 1800 cm^{-1} and the “CH region” in the range between 2700 and 3200 cm^{-1}. These two different spectral regions need clearly different filter setups according to the excitation scheme used and the corresponding CARS wavelength expected.

Moreover as it was already noticed, it is important to have the right dichroic mirror in the microscope scanning unit that reflects the excitation sources and transmits the generated signals on the sample to obtain also CARS epi-detection. Choosing the right dichroic mirror was not easy because of the particularity of the excitation wavelengths. Using for example the signal-idler excitation scheme, the dichroic mirror should reflect optimally in the range between 900 and 1300 nm and transmit all the wavelengths shorter than 900 nm. However this condition that is purely theoretical, since it is not possible to have a dichroic mirror with that steep edge transition, it is not enough to cover all the “fingerprint region” from 500 to 1800 cm^{-1} allowing just a detection from about 1200 to 3200 cm^{-1}. From these considerations it is clear that more dichroic filter types are needed to cover the entire ideal spectral window, as well as more optical filter types to be placed in front of the PMT.

The excitation signals are several orders more intense than the expected CARS signal, thus it is extremely important to attenuate strongly the excitation sources without attenuating the contrast signals. The PMT chosen has a sensitivity curve versus operation wavelength that shows a lower efficiency beyond 850 nm that decays at zero for longer wavelengths. This also helps to eliminate the excitation signals from the

detected signal, although this feature limits also the detection in the "fingerprint region" for both excitation schemes. Another type of detector is needed to perform optimal detection in the fingerprint region.

At this purpose it has been acquired a fast PIN Si photodiode biased photodetector (DET36A, Thorlabs), that has sensitive spectral range between 350 nm and 1100 nm with a maxima around 980 nm.

Filters selection was not easy since CARS microscopy is still a microscopy technique under development and it is spread among scientific laboratories around the world only at research level. Moreover as it was previously said there are several possible set-ups to realize CARS microscopy that make use of laser sources with different wavelengths. Custom-made filters sometimes are really expensive, so a trade-off between the ideal filter and the filters that are commercially available is necessary.

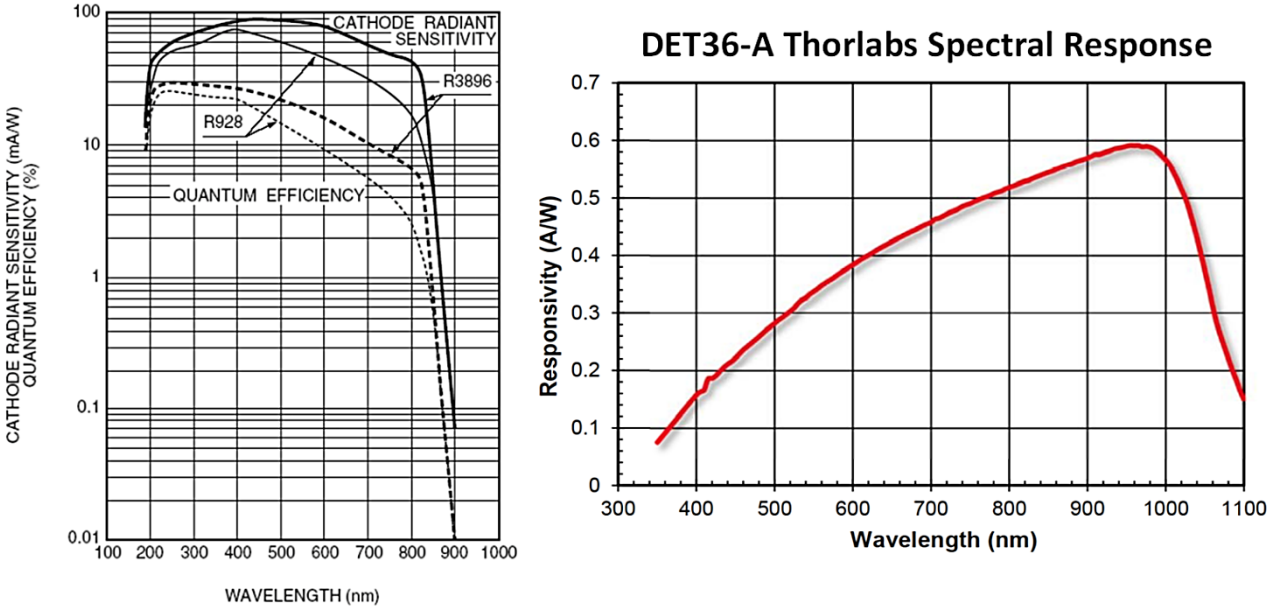

Fig. 3.30 Sensitivity curves of the detector chosen for multimodal microscopy. PMT Hamamatsu R3896 sensitivity (left). Fast response photodiode Thorlabs DET-36A (right).

With this knowledge several filters have been acquired and different combinations of them could be composed for both excitation schemes (Table 3.1).

At this step in order to consider only the filtering effect before the detector, the dichroic mirror was not considered.

With all the acquired filters it is possible to cover a spectral range between about 700 and 3400 cm^{-1} with signal-idler excitation scheme and a spectral range between about 500 and 3400 cm^{-1} with signal-1064 excitation scheme.

However, how it can be deducted from Fig. 3.31 and 3.32 and tables 3.2 and 3.3, it is not possible to cover the whole spectrum with a single combination of filters. For the "CH region" (between 2750 and 3100 cm^{-1}) if signal and idler are used as excitation source, the shortpass filters SP770, SP800 and SP810 combined with the bandpass filter FF01-716-43 could be used (CARS signal between about 700 and 730nm). If instead 1064nm output and signal are used as excitation sources, the shortpass filters SP700, SP770 and SP800 combined with the bandpass filter D660-60M could be used (CARS signal between about 630 and 690nm).

Producer	Model Type	Short name used
Chroma Technologies	ET890/220M	P890-220
Chroma Technologies	E870SP	SP870
Chroma Technologies	HQ875/75M	HQ875/75
Chroma Technologies	HQ960SP	SP960
Chroma Technologies	E920SP	SP920
Chroma Technologies	D455/70x	D455-70x
Chroma Technologies	ET405/20x	ET405-20x
Chroma Technologies	D480/30x	D480-30x
Chroma Technologies	D880/40M	D880/40
Chroma Technologies	ET810/90M	ET810/90M
Chroma Technologies	E950SP-2P	SP950
Chroma Technologies	D660/80M	D660-80M
Chroma Technologies	E700SP-2P	SP700
Semrock	FF01-716/43	FF01-716-43
Semrock	FF01-770SP	SP770
Semrock	FF01-531/22	FF01-531-22
Semrock	FF02-809/81	D809-81
Omega optics	970DCSPXR	DM970
Omega optics	850DCSPXR	DM850

Table 3.1 List of the selected optical filters with the short name used in the description of the setup.

For such regards the "fingerprint region" it is not possible to cover the entire spectral window with a single filter combination.

Using the signal-idler excitation scheme simplifying the filters used, the region could be divided in three major spectral parts:

- From about 750 cm^{-1} to 1000 cm^{-1} using the shortpass filters HQ960SP and E950SP-2P.
- From about 1000 cm^{-1} to 1700 cm^{-1} using the shortpass filters HQ960SP, E950SP-2P and E920SP with the bandpass filter HQ875/75 (bandpass filter D880/40 could be added to further block signal outside the spectral window in the range between 1150 and 1450 cm^{-1}).
- From about 1600 cm-1 to 2000 cm-1 using the shortpass filters HQ960SP, E950SP-2P, E920SP and E870SP with the bandpass filters ET810/90M and FF02-809/81

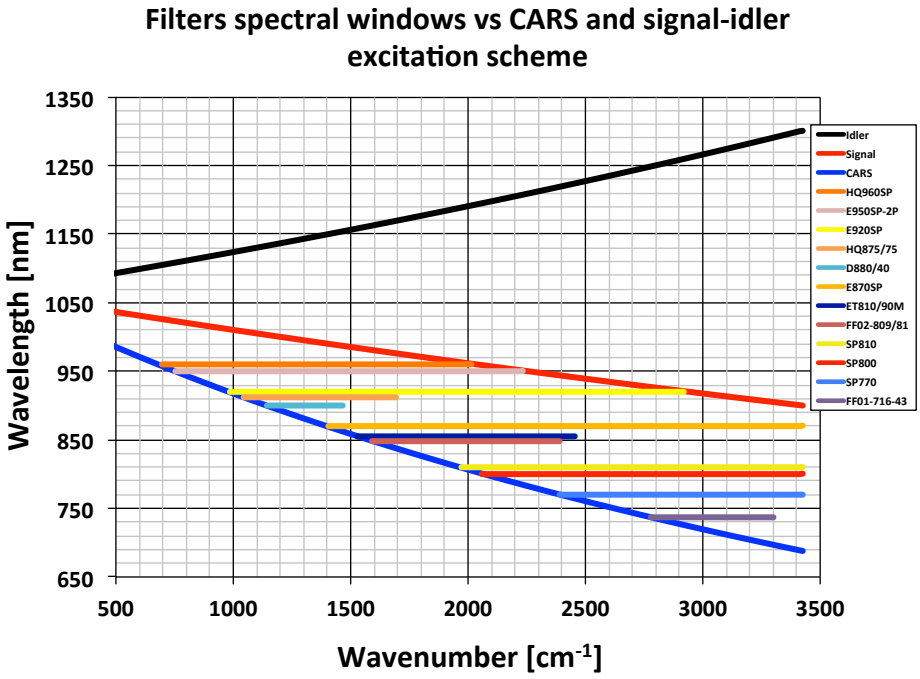

Fig. 3.31 Filters spectral windows versus CARS and signal-idler excitation scheme

Spectral Range [cm^{-1}]	Shortpass filter	BandPass filter
700 - 750	SP960	
750 - 1000	SP960, SP950	
1000 - 1050	SP960, SP950, SP920	
1050 - 1150	SP960, SP950, SP920	HQ875/75
1150-1500	SP960, SP950, SP920	HQ875/75, D880-40M
1500-1600	SP960, SP950, SP920, SP870	HQ875/75, ET810/90M
1600-1700	SP960, SP950, SP920, SP870	HQ875/75, ET810/90M, D809-81
1700-2000	SP960, SP950, SP920, SP870	ET810/90M, D809-81
2000-2200	SP950, SP920, SP870, SP810, SP800	ET810/90M, D809-81
2200-2400	SP920,SP870, SP810, SP800	ET810/90M, D809-81
2400-2750	SP920, SP870, SP810, SP800, SP770	
2750-2950	SP920, SP870, SP810, SP800, SP770	FF01-716-43
2950-3300	SP870, SP810, SP800, SP770	FF01-716-43
3100-3450	SP770, SP700	D660-80M

Fig. 3.32 List of the filter set combinations over the CARS spectral range for signal-idler excitation scheme.

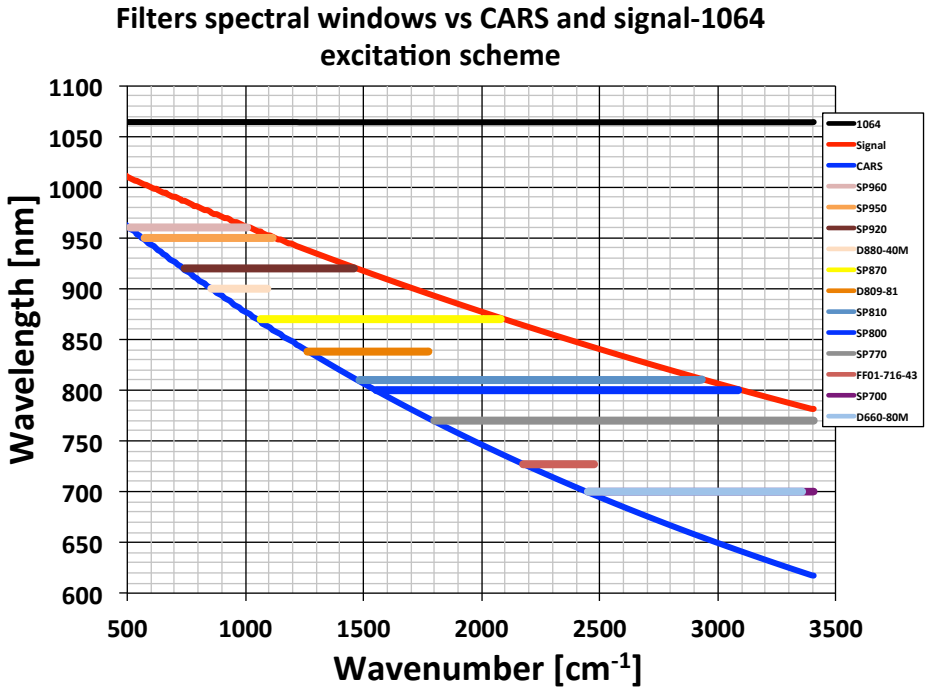

Fig. 3.33 Filters spectral windows versus CARS and signal-1064excitation scheme

Spectral Range [cm^{-1}]	Shortpass filter	BandPass filter
500 - 550	SP960	
550 - 750	SP960, SP950	
750 - 850	SP960, SP950, SP920	HQ875/75
850 - 1000	SP960, SP950, SP920	HQ875/75, D880-40M
1000-1100	SP950, SP920	HQ875/75, D880-40M
1100-1250	SP920, SP870	
1250-1450	SP920, SP870	D809-81
1450-1800	SP870, SP810, SP800	
1800-2100	SP870, SP810, SP800, SP770	
2100-2200	SP810, SP800, SP770	
2200-2500	SP810, SP800, SP770	FF01-716-43
2500-2950	SP810, SP800, SP770, SP700	D660-80M
2950-3100	SP800, SP770, SP700	D660-80M
3100-3450	SP770, SP700	D660-80M

Table 3.2 List of the filter set combinations over the CARS spectral range for signal-1064 excitation scheme.

Using the signal-1064 excitation scheme the "fingerprint region", simplifying the filters used, it could be also divided in spectral parts:

- From about 550 to 850 cm^{-1} using the shortpass filters HQ960SP, E950SP-2P.
- From 850 to 1100 cm^{-1} using the shortpass filters E950SP-2P and E920SP with the bandpass filter HQ875/75 and D880/40M.
- From 1100 to 1450 cm^{-1} using the shortpass filters E920SP and SP870 (adding the bandpass filter D809-81 between 1250 and 1450 cm^{-1} to further block unwanted signals).
- From 1450 to 1800 cm^{-1} using the shortpass filters SP870, SP810 and SP800.

Scan head and dichroic mirrors

In sample imaging the excitation sources are scanned over the specimen using the Olympus FV300 scan head. The scan head is composed by:

- Two galvanometric mirrors that scan the laser on the sample;
- An excitation dichroic mirror that reflects the excitation source towards the sample and transmits the generated signal from the sample;
- A pin-hole that works as confocal aperture to spatially filter the out of focus signal coming from the sample;
- An emission dichroic mirror to separate the emission spectrum in the two detection channels;
- A set of filters in the two branches of the detection channels;
- One PMT for each of the two detection channels.

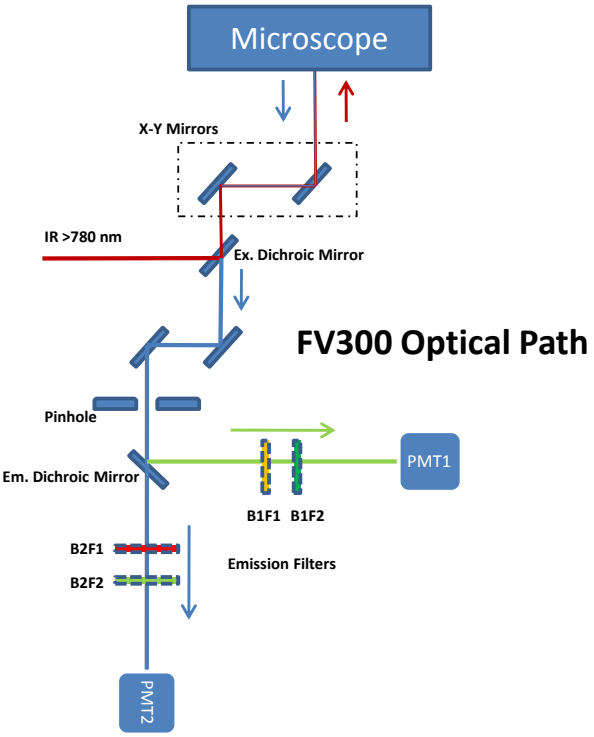

Fig. 3.34 Optical scheme of the Olympus FV300 scan head.

The scan unit allows, through the excitation dichroic mirror, the epi-detection of the generated signals from the sample.

The selection of the dichroic mirrors is not easy because it is impossible to find a single dichroic mirror suitable for epi and forward detection over the whole spectral region between 500 to 3400 cm^{-1} using both excitation schemes. Moreover a common feature of the dichroic mirrors is the presence of a transition spectral region that could extend for tens on nanometres, between the transmission and the reflective behaviours in which the dichroic mirror behaves like a beam splitter. The beam splitter behaviour of a dichroic mirror is generally an unwanted characteristic because it underperforms both the transmission and the reflection behaviour, attenuating both excitation and emission signals.

The ideal dichroic mirror in a multimodal CARS microscopy should excite the sample in the infrared region with the maximum efficiency and it should also allow detecting broadband spectra in the visible region in order to add also TPEF and SHG to CARS microscopy.

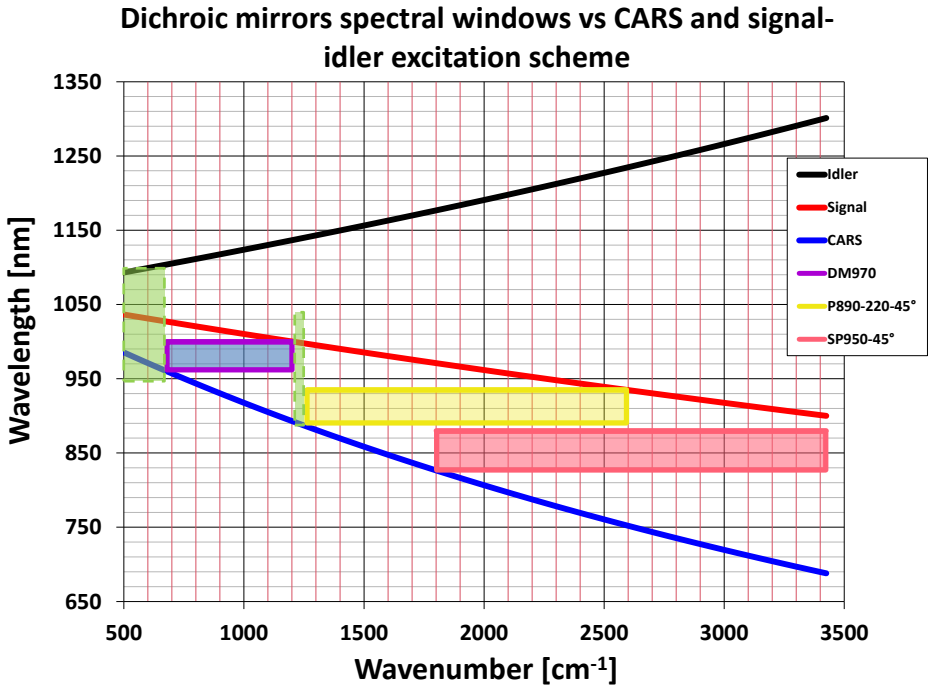

Fig. 3.35 Dichroic mirrors spectral windows versus CARS and signal-idler excitation scheme.

Some of the dielectric filters used to select the detected spectral window can be also used as dichroic mirror if tilted by 45°. In dielectric filters the amount of reflected light is nearly completely transmitted since almost no power is absorbed by these kinds of filters. The filter spectral transmittance/reflectivity changes with the tilting angle because the optical path length between the dielectric layers of the filter changes accordingly.

In order to use optical filter instead of classic dichroic mirror imposed to design and realize a dichroic mirror mount to be place in the Olympus FV-300 scan unit (Fig. 3.36).

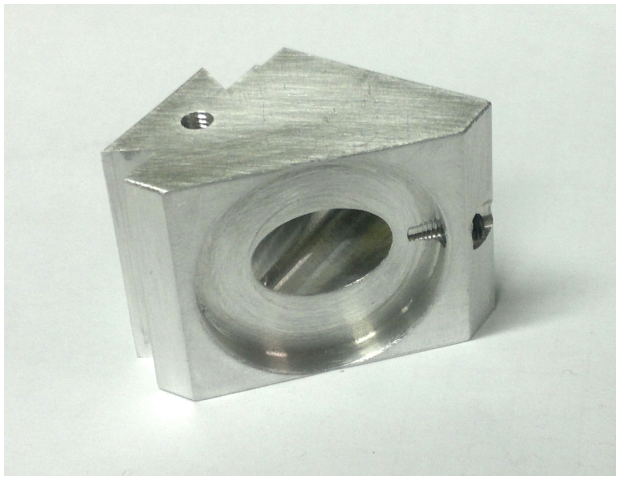

Fig. 3.36 Dichroic mirror mount for round filters to be placed in the FV300 scan head.